Kinematic SAMI : a new real-time multi-sensor data assimilation strategy for nonlinear modal identification

Adrien Goeller, Jean-Luc Dion, Ronan Le Breton, Thierry Soriano

Mechanics & Industry **21**, 413 (2020)
© AFM, EDP Sciences 2020
https://doi.org/10.1051/meca/2020035

Mechanics & Industry

Available online at:
www.mechanics-industry.org

REGULAR ARTICLE

Kinematic SAMI : a new real-time multi-sensor data assimilation strategy for nonlinear modal identification

Adrien Goeller[1,*], Jean-Luc Dion[1], Ronan Le Breton[2], and Thierry Soriano[3]

[1] QUARTZ-SUPMECA – Institut Supérieur de Mécanique de Paris, 3 rue Fernand Hainaut, 93400 Saint-Ouen, France
[2] Univ Rennes, INSA Rennes, LGCGM - EA 3913, F-35000 Rennes, France
[3] Université de Toulon, Bâtiment M, CS 60584, 83041 Toulon CEDEX 9, France

Received: 22 February 2019 / Accepted: 5 April 2020

Abstract. In many engineering applications, the vibration analysis of a structure requires the set up of a large number of sensors. These studies are mostly performed in post processing and based on linear modal analysis. However, many studied devices highlight that modal parameters depend on the vibration level non linearities and are performed with sensors as accelerometers that modify the dynamics of the device. This work proposes a significant evolution of modal testing based on the real time identification of non linear parameters (natural frequencies and damping) tracked with a linear modal basis. This method, called Kinematic-SAMI (for multiSensors Assimilation Modal Identification) is assessed firstly on a numerical case with known non linearities and secondly in the framework of a classical cantilever beam with contactless measurement technique (high speed and high resolution cameras). Finally, the efficiency and the limits of the method are discussed.

Keywords: Experimental modal analysis / Extended Kalman Filter / Data Assimilation / Nonlinear identification / Real-time

1 Introduction

Measurements in structural dynamics are used to identify and update models in order to determine the stability, safety and lifetime of mechanisms under operational or exceptional conditions. In many cases, this experimental process is developed in the scope of modal analysis. Modal analysis is a very well-known tool which consists in measuring input and output signals in order to define the studied system in terms of modal parameters (natural frequencies, damping ratio and mode shapes) [1]. Modal parameters are often identified in the frequency domain from Experimental Modal Analysis (EMA) techniques by using the Frequency Response Functions (FRF) and this method solves efficiently many problems [2].

In experimental modal analysis, experiments are often performed using a limited number of measurement points. These measurement points are mostly acquired using accelerometers. The presence of these sensors on the studied structure induced some drawbacks. First, the added mass effect induced by the sensors located on the structure can affect its natural frequencies and mode shapes. Moreover, wires used to connect sensors to the acquisition systems modify the measured modal damping. These drawbacks and the limited number of measurement points are successfully avoided in many studies with laser measurements [3,4]. However, this technique is based on sequential scanning method and need to study the dynamics of structures with periodic or repeated deterministic responses. Transient and random excitation cannot be studied with this technique by measuring all points in the same time. The commonly used solution consists in reproducing the same excitation (transient or pseudo random) for each measured point. However, the experimental process is yet much longer and numerous assumptions are required: the system is assumed to be deterministic and stationary and measurements have to be synchronized.

The motivation of this work is to tackle these drawback. Part of the solution consists in using contactless devices such as laser, micro wave, or high speed vision. The purpose of this article is to introduce a new real-time method which is able to identify nonlinear modal parameters using a large number of observation points from different contactless sensors input.

In most of the recent methods modal parameters are assumed to be obtained from a linear structure. However, for industrial structures such as aircraft, space launchers, bridges, but also for smaller structures like brakes or ski, weak non linearities can be observed even for small vibration levels. These weak non linearities modify

* e-mail: adrien.goeller@supmeca.fr

natural frequencies and modal damping which depend on the vibration level. There are methods, most of them based on the work of Kerschen et al. [5]. These methods require significant computation times. In many industrial studies, Numerical Modal Analysis are more and more performed before Experimental Modal Analysis. Thus, expected frequencies, damping and mode shapes are used to optimize experimental parameters in the acquisition system, sensors and measurement point location.

The present study aims to identify in real time nonlinear modal parameters in the case of weak nonlinearities. The Kinematic model used is based on the numerical modal basis and is assumed to not depend on vibration amplitude. We propose to use the framework of data assimilation. Data assimilation is a family of methods which allows to use a model with data in a stochastic framework [6].

In order to perform real time identification, we use a sequential assimilation method known in the signal processing domains as Kalman filters. This work is specifically focusing on nonlinear Kalman filters. Firstly introduced in the early sixties [7], this promising technique for estimation with a linear model designed by Rudolf Kalman was not well accepted [8] but quickly became a very used algorithm until now. Not to ease the bibliographic work, the filter has been improved in a lot of different way and domains, in order to deal with a large variety of problems. Indeed, Kalman filter is not only the original algorithm, but also it has become a family of algorithms. In order to go beyond the linear framework of the Kalman filter, Stanley Schmidt developed in a NASA context an Extended Kalman Filter (EKF) [9] developed decades later in a civil context [10] based on a linearization of a nonlinear model. From this filter has derived a lot of references on multiple domains: ballistic, chemical reactions control, aerospace, robotic [11,12]. In the particular field of dynamics, EKF has been widely used for tracking specific model parameters in order to do health monitoring [13]. In the EMA framework, linear Kalman filter was used to estimate simulated vibrating forces [14] following by the EKF for estimating simulated input forces acting on structural systems [15]. Other approaches use data driven stochastic subspace identification (SSI-DATA) in order to mix computational and structural parameters in the identification results. The disadvantage of the SSI methods is the use of computational resources, which is difficult to transpose in a real time framework.

Frequency tracking is not a new trend. The real time framework, the objectives of non linear identification and the expected time-frequency accuracy stop us from using Fourier Analysis Methods. But this framework has been tackled with Auto Regressive Moving Average (ARMA models) [16,17] with a drawback on the complexity and robustness of the identification process in the case of nonlinear systems. Different methods from the optimal estimation framework [18] are already employed to track frequency. For example a monitoring vibration approach is applied on a gearbox, providing alert indicators using an EKF coupled with autoregressive models [19]. The system is robust and effective to identify optimal model order. However some false alerts are generated by this method and the system is not designed to use the whole modal information. The specific topic of modal parameters estimation is very dynamic and a lot of different recent works use the optimal estimation framework.

Nowadays, some authors points out the importance of the experimental extraction of nonlinear modes to model systems or characterize the system dynamic [20]. Yang et al. [21] is using high speed videos of structures with a video magnification to amplify the displacement. Then, a blind source separation is performed to extract the modal parameters, but in a linear context. Abdollahpouri et al. [22] compare EKF and Moving Horizon Estimation to tackle real time estimation but the estimation is limited to one mode. Dzunic et al. [23] use Bayesian State-space (BSS) approach to estimate the probability of defect occurring in a structure. The BSS formalism can be used in real-time, but the computation of the probability distributions is expensive. Nonlinear version of Kalman filters needs less computational time. Using those promising methods, Naets et al. [24] use an EKF for identifying forces input in a structural system using a classical random walk model. This approach implements directly a discretized version of the classical differential system as a model and follows the framework developed by Chatzi [13] in the structure health monitoring field. The results propose only the estimation of the force.

A different approach using Kalman filtering consists in performing a modal demodulation model in the EKF for accurate measurements of non stationary natural frequencies and modal damping [25]. However observations are based on 1D sensors and the proposed algorithm is built on Extended Kalman Filter Series, with no link to the structure and its eigenvector basis. Cha et al. [26] use another nonlinear version called Unscented Kalman Filter and a model of the expected signal response to estimate structural properties of the structure and the input force. This approach does not use a modal context which allows several modes estimation and even if the model used is nonlinear, the estimation is performed on a linear structure. Other recent approaches use demodulation techniques with neural networks to identify nonlinear modes but for a single frequency response function [27].

The proposed method based on sequential data assimilation is developed in Section 2 with the description of the modal model generalized in a EKF for N-Dimensional observations. The purpose of this article is to develop a real time modal analysis for weakly nonlinear structures based on an EKF and fused contactless measures. On the tracks of identification with sequential data assimilation as Kalman filters using nonlinear models [28], we use a modal framework for modeling the input data. The method presented in this article is at the centre of the measurement/processing chain. It allows in the targeted applications to combine different types of sensors while offering fast information processing.

The system is able to identify in a real time scheme the different nonlinear parameters of a structure modal model for each vibration eigenmode and for transient observations: frequency, magnitude and damping. It is using a Reduced Order Model based on the modal basis of the structure. The experimental procedure is using data from

high speed camera and laser. The application test cases are described in Section 3 with a validation on a numerical test case and an experimental one with geometrical nonlinearities. Finally, in Section 4 both numerical and experimental results are given for nonlinear simulation and discussed for the nonlinear simulation and the real measurements acquired with the experimental setup.

2 Sequential assimilation in a modal framework

Data assimilation is very well described by the elegant formula from the geoscience fields: "Data assimilation is the science of successful compromises" [6], compromises between both simulation and experimental worlds. Developed since the thirties in the meteorology field, these methods are generating an increasing interest in a lot of different domain following the data driven philosophy.

Data assimilation groups two main types of methods:

- Variational methods use data on an interval including past and future information regarding the time where estimation is performed. The most used method in this case is the 4D-Var method [29].
- Sequential methods use only past information. These methods are based on Kalman filters algorithms to assimilate the model with data.

The Extended Kalman Filter, as described in Dion et al. [25] is robustly designed to track sine component signals. In order to adapt the method to N-dimensional measurement, we have to set up a spatial relationship between the different observed points according to the time vision of the sinus tracking. Section 2.1 describes the system of equations. Extended Kalman Filter equations and state system employed are introduced in Section 2.2 and Section 2.3.

2.1 Modal model in a weak nonlinearity framework

A vibrating system can be written as :

$$M\ddot{x} + C\dot{x} + Kx + F_{NL}(x, \dot{x}) = F_{ext} + \nu. \tag{1}$$

These equations describe the time and space relations for the general coordinates of the system described by their position x, speed $\dot{x}$ and acceleration $\ddot{x}$. M is the mass matrix, K and C are the stiffness and damping matrix. F_{ext} is modeling the external forces and F_{NL} the nonlinear forces depending on position and speed. ν is modeling the uncertainty of the model. This uncertainty is assumed to be unbiased and Gaussian, with zero means and a covariance matrix R_ν.

In the linear context of modal analysis the deterministic system can be written in the frequency domain as:

$$\begin{aligned}&(-\omega^2\Phi^T M\Phi + j\omega\Phi^T C\Phi + \Phi^T K\Phi)\cdot\hat{q} = \Phi^T\hat{F}_{ext}\\ &\text{with } \hat{x} = \Phi\hat{q}.\end{aligned} \tag{2}$$

The solutions of the system (Eq. (2)) can structurally be decoupled in time and space. Thus, the solution can be decomposed on a modal basis depending on the structure $\Phi = \left\{\Phi^1, \Phi^2, ..., \Phi^n\right\}$ depending only on the space. The mode index $i \in [\![1, ..., n]\!]$ is in superscript for the consistency of the following. Different important underlying hypotheses have to be pointed out:

- At any time, the shape function is a linear combination of mode shapes.
- Instantaneous natural frequency and damping depend on the modal amplitude of the corresponding mode.

From those, two important assumptions can be made:

- The modal base used is assumed to be strictly real (without any phase between nodes for each natural mode).
- The system is in the weak nonlinear framework [30]: the eigenvectors are assumed to be time invariant.

In the case of free oscillations, the solution can be written as a shape function $S(x, y, z, t)$ under the form:

$$S(x, y, z, t) = \sum_{i=1}^{n} V^i(t)\cdot\Phi^i(x, y, z) + \nu \tag{3}$$

$$\text{with } V^i(t) = A^i(t)\cdot\cos\left(2\pi\cdot\int_0^t f^i(\tau)d\tau + \phi^i\right) \tag{4}$$

$$A^i(t) = a^i\cdot \mathrm{e}^{-2\pi\cdot f^i(t)\xi^i(t)t} \tag{5}$$

$$\nu = \sum_{i=n+1}^{\infty} V^i(t)\cdot\Phi^i(x, y, z) + \mu. \tag{6}$$

In the previous equations $f^i(t)$ is representing the frequency, ϕ^i the phase, $\xi^i(t)$ the damping and a^i the initial mode coefficient for mode i. ν includes the uncertainty of the model but also the rest of the modal basis in the case of a truncated modal basis (reduced order model). We call ν the residual and we verify in the last section that this residual model given in the above equation is verified. μ is modeling the uncertainty.

The model and observation function derive from this general model and are given in Section 2.3 while the Kalman framework is introduced first in Section 2.2.

2.2 The extended Kalman filter

This section describes assumptions and the retained set of equations for the Kalman filter. Let's consider a classical nonlinear state system with a time evolutive equation and an observation equation:

$$\begin{cases}\dot{x}(t) = f_c(x(t)) + w(t)\\ z(t) = h_c(x(t)) + v(t)\end{cases} \text{ or in a discrete form:}$$

$$\begin{cases}X_{k+1} = f(X_k) + w_k\\ Z_k = h(X_k) + v_k.\end{cases} \tag{7}$$

In these equations, X_k is the state vector at step k, mirroring the discrete version of the continuous state version

$x(t)$. The function f_c and its discretized version f models the system evolution with a process noise $w(t)$ or w_k. The function h_c or its discretized version h is the observation function. It links the state variable space with the measurement space with an observation noise $v(t)$ or v_k.

Kalman filters are part of the largest class of Data Assimilation algorithms. Data assimilation groups the methods used to fit models with real data in order to do prediction or identification. Kalman filters belong to the class of sequential algorithms and uses the two first statistical moments, the means and covariances of a variable vector X and an evolutive state system (Eq. (7)) to compare real data with an input model.

The original Kalman filter [7] estimates the probability distribution of X with the functions f and h defined linear (for the sake of clarity, f has no link with F_{NL} and F_{ext} introduced in Eq. (1)). Defining f_k and h_k two invariant matrix as $f(X) = f_k X$ and $h(X) = h_k X$, the linear equation can be expressed in a two-step process. First, the prediction step, which uses the evolution part of the equation (7) to predict an estimation of the future state for mean $\hat{X}_{k|k-1}$ and covariance $P_{k|k-1}$ based on their past state $\hat{X}_{k-1|k-1}$ and $P_{k-1|k-1}$

$$\hat{X}_{k|k-1} = f_k \hat{X}_{k-1|k-1} \tag{8}$$
$$P_{k|k-1} = f_k P_{k-1|k-1} f_k^T + Q_k \tag{9}$$

Kalman filter introduces Q_k, which is the covariance of the process noise w_k supposed to be Gaussian and centered.

The second step is the update, during which the prediction is compared to the observation using the observation part of the equation (7).

$$S_k = h_k P_{k|k-1} h_k^T + R_k \tag{10}$$
$$K_k = P_{k|k-1} h_k^T S_k^{-1} \tag{11}$$
$$\hat{X}_{k|k} = \hat{X}_{k|k-1} + K_k(z_k - h_k \hat{X}_{k|k-1}) \tag{12}$$
$$P_{k|k} = (I - K_k h_k) P_{k|k-1}. \tag{13}$$

These equations introduce K_k the Kalman gain and R_k the covariance of the observation noise v_k supposed to be Gaussian and centered. As we can see in equation (10), the strength of this class of methods is to use a gain driven by the covariances to adapt the state vector to the observations.

Unfortunately, the linear algorithm is not sufficient to characterize the distributions in nonlinear cases. The Extended Kalman filter tackles this problem by linearizing the functions at each step. It uses the nonlinear state equations (Eq. (7)) to propagate the means and introduces the Jacobian matrix F_k and H_k derived from the functions f and h linearized at step k to propagate the covariances.

The complete extended Kalman filter equations with linearization of the nonlinear functions f and h are then shown below.

$$\hat{X}_{k|k-1} = f(\hat{X}_{k-1|k-1}) \tag{14}$$
$$P_{k|k-1} = F_k P_{k-1|k-1} F_k^T + Q_k \tag{15}$$
$$S_k = H_k P_{k|k-1} H_k^T + R_k \tag{16}$$
$$K_k = P_{k|k-1} H_k^T S_k^{-1} \tag{17}$$
$$\hat{X}_{k|k} = \hat{X}_{k|k-1} + K_k(z_k - h(\hat{X}_{k|k-1})) \tag{18}$$
$$P_{k|k} = (I - K_k H_k) P_{k|k-1}. \tag{19}$$

The Extended Kalman Filter has several drawbacks. Its implementation is not easy because of the complexity of the jacobian calculus. The jacobian drives up the computational cost of the EKF compared to a standard Kalman for example. Another drawback caused by the linearization of the model is the robustness in the case of high nonlinearity. Indeed EKF induces process errors because of the difference between the curve and the linearized projection: those errors grows with the nonlinearity of the function for a fixed step.

Those errors are also important to tune the filter. The initialization is not difficult. The P_0 matrix is defined diagonal with the squared variance for each state variable. It can be easily transposed by the experimenter as an error interval allowed around the chosen X_0 value. The R_k value is defining the confidence on observation. It can be linked with the precision of observations in the same way than the P_0 value. Q_k value represents the error of the model. This error includes linearization error and modeling error.

Section 2.1 describes the modal analysis framework. The model is based on an invariant (linear) modal basis and is designed in order to track weak nonlinearities that are observed through the evolution of the natural frequencies and damping. These weak nonlinearities of the model allow to use EKF: only natural frequencies and modal damping are time varying. Moreover amplitude and frequency variations are assumed to be much slower than studied vibrations: observed signals can be depicted as narrow band signals.

Section 2.3 describes the state system derived from the modal model in Section 2.1 and used to track modal parameters of a structure.

2.3 State system

This section introduces the design of the state system used in the EKF algorithm.

The design of the evolution function matrix has been defined by Dion et al. [25] for the tracking a sine components in a signal. The general form of the solution given in equation (3) can be split in two parts: a time part and a space part. For the specific mode i, the time part is defined as:

$$V^i(t) = A^i(t) \cdot \cos\left(2\pi \cdot \int_0^t f^i(\tau) d\tau + \phi^i\right) \tag{20}$$

A common solution to model the signal is to use analytic signal based on the Hilbert transform. However the

Hilbert transform induces some bias when implemented and the approximation is correct only under the Bedrosian theorem first condition [31], which is commonly called conditions of narrow band signal. This assumption is often well defined in telecommunication domain, but can be more tricky in identification or tracking for complex signals [32]. This issue is a current investigation question, and recent works try to extend the Hilbert transform without the Bedrosian condition [33]. In our case, amplitude and frequency evolutions given in equation (20) are slow considering the signal, which allows to satisfy the narrow band conditions.

In other terms, studied signals can be described with in equation (20):

$$V^i(t) \simeq A^i(t) \cdot \cos\left(2\pi \cdot \int_0^t f_p^i(\tau) + f_\Delta^i \cdot m(\tau) \cdot d\tau\right) \tag{21}$$

$$\text{with } f^i(t) \simeq f_p^i + f_\Delta^i \cdot m^i(t) \tag{22}$$

$$f_\Delta^i << f_p^i \tag{23}$$

$$|m(t)| < 1. \tag{24}$$

Following the narrowband definition, we define the carrier and phase frequencies f_p^i and f_Δ^i for the ith mode. The $m(t)$ function represents the bandwidth modulation of the signal. This amplitude and frequency modulations implies a last condition already verified regarding the definition given in equation (3), but important to mention:

$$\frac{dA^i(t)}{dt} \ll 2\pi \cdot f_p^i(t). \tag{25}$$

In a first approach, the pseudo harmonic signal can be set into an analytical signal with the following discrete version (the imaginary part is the Hilbert transform of the original signal):

$$\mathcal{V}_k^i = \alpha_k^i \cdot \mathrm{e}^{j2\pi f_k^i k \cdot \Delta t}. \tag{26}$$

Considering that the parameters α^i and f^i are varying slightly over time:

$$\mathcal{V}_{k+1}^i \simeq \alpha_k^i \cdot \mathrm{e}^{j2\pi f_k^i (k+1)\Delta t}. \tag{27}$$

Then, we have the following state form :

$$\mathcal{V}_{k+1}^i \simeq \mathcal{V}_k^i \cdot \mathrm{e}^{j2\pi f_k^i \Delta t}. \tag{28}$$

Separating real part and imaginary part:

$$\mathcal{V}_k^i = V_k^i + j \cdot \widetilde{V}_k^i. \tag{29}$$

The state system becomes:

$$\begin{pmatrix} V_{k+1}^i \\ \widetilde{V}_{k+1}^i \end{pmatrix} = \begin{bmatrix} \cos(2\pi f_k^i \Delta t) & -\sin(2\pi f_k^i \Delta t) \\ \sin(2\pi f_k^i \Delta t) & \cos(2\pi f_k^i \Delta t) \end{bmatrix} \begin{pmatrix} V_k^i \\ \widetilde{V}_k^i \end{pmatrix}. \tag{30}$$

If we take into account the frequency modulation, the state system becomes with notation from Section 2.2:

$$X_k^i = F_{k-1}^i \cdot X_{k-1}^i \tag{31}$$

$$\text{with } X_k^i = \left[V_k^i, \widetilde{V}_k^i, \omega_k^i\right]^T \quad \omega_k^i = 2\pi f_k^i \Delta t \tag{32}$$

$$\text{and } F_k^i = \begin{pmatrix} \cos(\omega_k^i) & -\sin(\omega_k^i) & 0 \\ \sin(\omega_k^i) & \cos(\omega_k^i) & 0 \\ 0 & 0 & 1 \end{pmatrix}. \tag{33}$$

The evolutions of the amplitude $\alpha_k^i = \sqrt{V_k^{i^2} + \widetilde{V}_k^{i^2}}$ and the frequency are slow regarding the time step. The state system is nonlinear (Eq. (14)) and W_k the process noise is centered and Gaussian with its covariance defined as Q_k in Section 2.2.

The following space part of the state system is one of the key points introduce in this article. This part is significant to introduce multiple observations. These observations could come from multiple sensors or from processed digital images. The observation function link the modal variables of the state system to the observed measurements. These link is performed with the modal basis. The discrete form of the space is defined by the set of measurement points (sensors) such as $\Phi_p^i = \Phi^i(x_p, y_p, z_p)$.

To deal with n modes, we concatenate vertically the different modal variables and define the block matrix evolution as:

$$X_k = \begin{pmatrix} X_k^1 \\ X_k^2 \\ \dots \\ X_k^n \end{pmatrix} \text{ and } F_k = \begin{pmatrix} F_k^1 & 0 & \dots & 0 \\ 0 & F_k^2 & \dots & 0 \\ \dots & \dots & \dots & \dots \\ 0 & 0 & \dots & F_k^n \end{pmatrix}. \tag{34}$$

The observation from the sensors gives different discretized measures of shape functions $S_{k,p}$:

$$S_{k,p} = \sum_{i=1}^{n} V_k^i \cdot \Phi_p^i + \nu. \tag{35}$$

The observation function has to be designed in order to transform the state vector to the model space. This model space is defined by the equation (3): this is the sum of the n first modes contribution at each time step.

The modal basis is used in the observation equation in order to link the state variable with the measurements:

$$S_{k,p} = H \cdot X_k \tag{36}$$

$$= \sum_{i=1}^{n} V_k^i \cdot \Phi_p^i \tag{37}$$

$$\text{with} \quad H = \begin{pmatrix} \Phi^1 & 0 & 0 & \Phi^2 & 0 & 0 & \dots & \Phi^n & 0 & 0 \end{pmatrix}. \tag{38}$$

This new form is particularly designed for free vibrations of structures measured with la large set of sensors. The next section describes the implementation of the previous model.

3 Experimental setup

This section describes the experimental setup we use to validate the theoretical development of the previous part. First, the test case chosen to prove the feasibility of the theoretical concept is introduced: a classical cantiveler beam (Sect. 3.1). Then, the experimental setup is described in Section 3.2 in order to validate the Kinematic SAMI on a real test case. We choose to measure the cantilever beam with a high speed video acquisition.

3.1 Application on a case study: the cantilever beam

We propose an experimental application with contactless measurements of a structure with geometrical nonlinearity in the modal analysis framework. In order to test the different parts of the estimation process described below, an experimental validation on a classical cantilever beam is proposed. Only bending modes are studied which means that the beam is considered in the 2D plane (e_x, e_z) (see Fig. 1). According to the Euler Bernoulli theory, the bending motion is assumed to be only along the e_x axis and displacements along e_z axis are neglected. In order to deal with all the cases, three tests cases are presented:

1. A numerical simulation composed with 3 modes whose frequencies and damping are varying: the nonlinear case study. Three variables per mode will be identified along time: the modal magnitude, the damping coefficient and the frequency. One mode is hardening and two are softening ones.
2. A real test case described in the Section 3.2 and excited by a shock. Measurements are performed with a high speed camera and with specific marks on the beam. The camera position allows to neglect the depth and to consider the image processing of the beam in a 2D plane (Fig. 1). The evolution of the positions of each marker is extracted with a video processing algorithm.
3. In the same experimental test case, another sensor is added: displacement measurements measured with a laser on one point of the cantilever beam.

3.2 Experimental setup

The modal basis of the aluminium alloy beam is obtained in accordance with the Euler-Bernoulli theory.

Considering the 1D modal basis of this classical test case $\Phi = \{\Phi^1(x), \dots, \Phi^n(x)\}$, the cantilever beam solution $S(x,t)$ is:

$$S(x,t) = \sum_{i=1}^{n} V^i(t)\Phi^i(x) \tag{39}$$

Table 1. Properties of the cantilever beam.

Length	0.45 m
Height	0.02 m
Width	0.0012 m
Density	2700 kg m^{-3}
Young's Modulus	74 Gpa

Table 2. Theoretical frequencies of the cantilever beam modes.

Mode number	1	2	3	4	5
f (Hz)	4.17	10.43	17.45	24.43	31.41

The geometric and mechanical properties have been chosen regarding the number of modes expected in the observation. Table 1 presents the properties of the beam. The theoretical first five mode frequencies are given in the Table 2. The clamping is built with steel block (see Fig. 1), not as ideal as the Euler-Bernoulli assumptions. However, the displacement induced by the non ideal clamping is negligible compared to the bending displacement amplitudes observed.

In this first part, the experimental setup is composed of three elements:

- The high speed camera;
- the clamped free beam;
- the spotlight.

Using aluminum in the visual field brings a major disadvantage: its specular properties. Besides, there is no particular position of the light and the cantilever beam to avoid reflection stray light. This issue has been tackled by using specific pattern placed every centimeter and providing 45 observation points for the estimation (Fig. 1). The measures are extracted from the video using a specific method based on the tracking of interest points [34].

The camera is calibrated using the method proposed by Zhang [35] implemented in MATLAB. The pixel size projected on the experimental device (called Ground Sample Distance or GSD the remote sensing field) is 108×10^{-6} m and is presented in Section 4.4. The measures are processed by our algorithm and then compared to a classical Fourier analysis of each observation point.

4 Numerical investigations and experimental results

First Section 4.1 defines the criteria for evaluating the performance of the method and the tuning of the different parameters used.

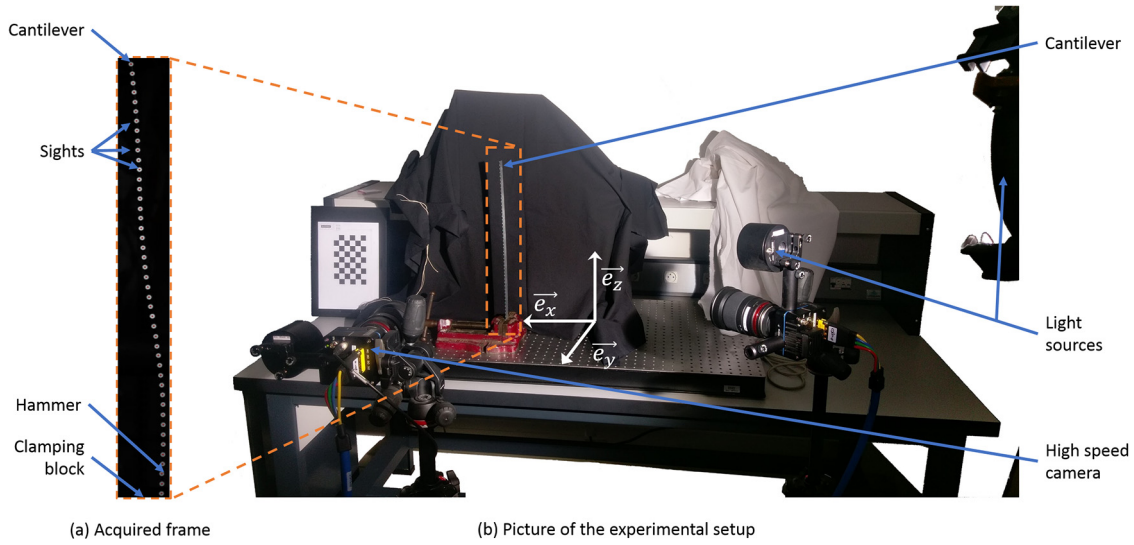

Fig. 1. Experimental setup.

4.1 Criteria for method evaluation

The model introduced in Section 3.1 is used to simulate a numerical test bench. This linear model is computed in order to extract mode shapes. The assumption of weak nonlinearities allows using these modes shapes with nonlinear natural frequencies and dampings. Then a nonlinear simulation is proposed, introducing variations of the frequencies (as introduced in Eq. (3)). An important noise is added on observations in order to generate a realistic and severe test for the proposed method. This noise is satisfying two hypothesis: the noise is considered Gaussian centered and the noise is considered to be additive.

To quantify the convergence of the filter, the error will be measured regarding each variables. A classical Root Square Mean Error (RMSE) residual estimator is used:

$$\mathrm{RMSE} = \sqrt{\frac{\sum_{k=1}^{k_{\mathrm{end}}} (V_{k_{\mathrm{estimated}}} - V_{k_{\mathrm{simulated}}})^2}{k_{\mathrm{end}} \cdot \Delta t}}. \quad (40)$$

Indeed, the RMSE gap between the acquisition data and the model output projected on the observation space is very common in the Data Assimilation domain. In our case, we compute a ratio between RMSE and the measures in order to compare the different extracted modes through a percent value. For example for the frequency:

$$f^i_{\mathrm{error}} = \sqrt{\frac{\sum_{k=1}^{k_{\mathrm{end}}} \left(f^i{}_{k_{\mathrm{estimated}}} - f^i_{k_{\mathrm{simulated}}}\right)^2}{k_{\mathrm{end}} \cdot \Delta t \cdot f^i_{k_{\mathrm{simulated}}}}} \times 100. \quad (41)$$

The constant parameters are extracted from the final value of the output filters and compared to the ground truth value in the case of the simulations. Finally, a special attention is focused on the residual for the real case. According to the modal decomposition in equation (3), it is interesting to show that the residual is composed of the sum of the non identified modes and the noise.

We choose to test the algorithm on a usual case of 3 modes identification. The simulation is based on the theoretical modes given in the Table 2. The performed during 5 s with a time step of $\Delta t = 5 \times 10^{-6}$ s . A white and Gaussian noise (standard deviation $\sigma_{\mathrm{sim}} = 200 \times 10^{-6}$ m) is added to the model equation (39) used to simulate the beam shape evolution over time. The spatial frequency is chosen very high for the ground truth with 1000 points, whereas the spatial frequency of the data simulated for the filter input is sampled to 25 points. The algorithm is calibrated first on a linear test case with constant frequencies.

4.2 Nonlinear numerical case study

Nonlinearities are introduced on natural frequencies and dampings. Three modes are studied, one mode is hardening and two are softening nonlinearities are larger than classical structures in order to assess the method used.

The results are presented in Figure 2. The simulation values of the reference variables are in a red dash-line. The identified variables are in blue continuous line. Multiples of the covariances are in green around the different parameters.

The results are convincing: the identification process is able to track the frequency and the envelop in a real time scheme. The envelop gives access to the time evolution of the damping coefficient, which allows to characterize completely the observed structure. Moreover, it is interesting to point out that the covariance evolves on the opposite expected behavior: instead of converging, the covariance seems to grow with time. The different modes amplitude are decreasing, generally as fast as the mode number is high. The filter confidence in the higher modes is then decreasing with time due to the observed amplitude become smaller and is coming closer to the noise, which explains the increasing covariance.

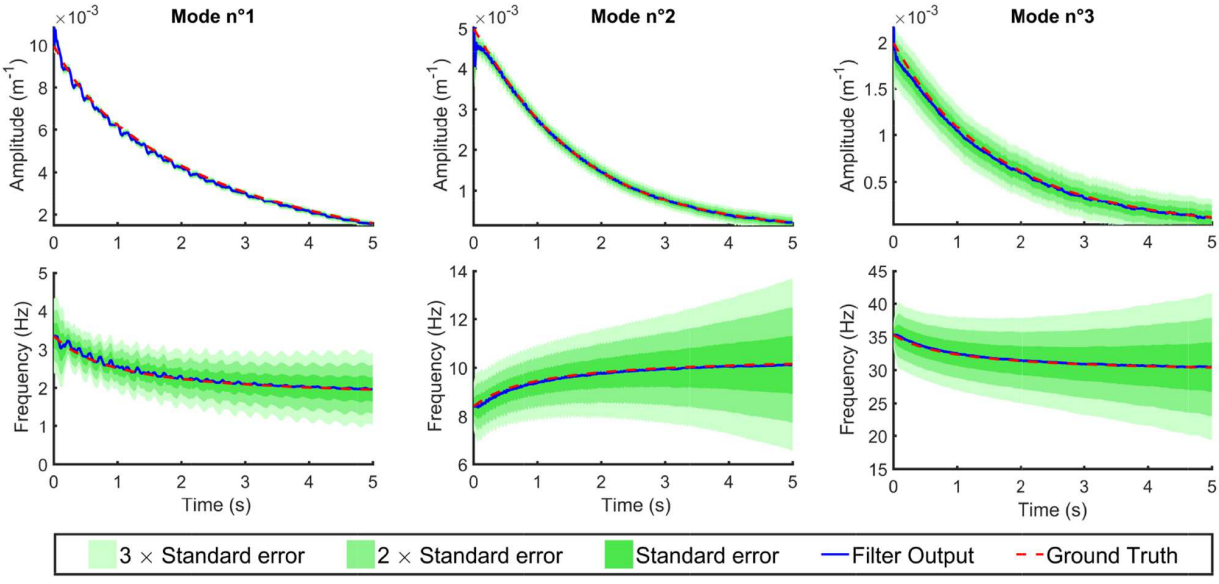

Fig. 2. Results for identification on a nonlinear case study.

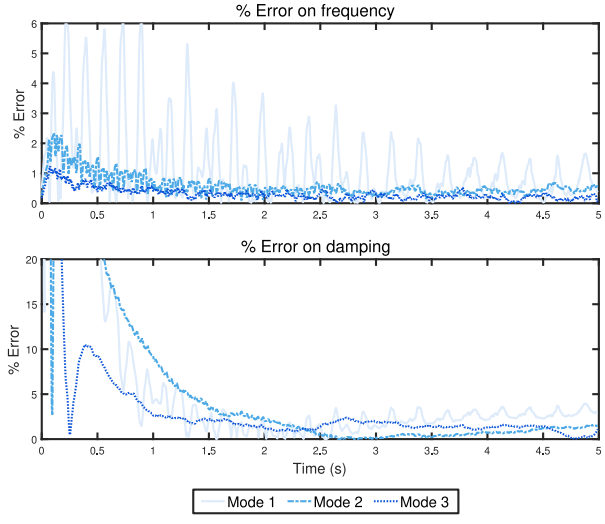

(a) Evolution of error for identification on a nonlinear case study

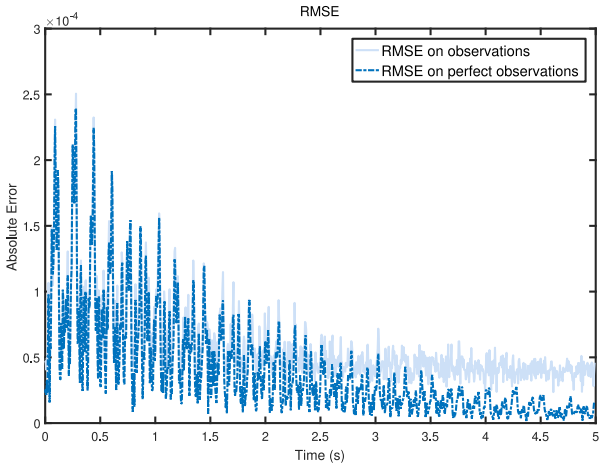

(b) RMSE ratios for identification on a nonlinear case study in case of noisy observation and perfect measurements

Fig. 3. Error evolution for each mode of the real time identification of the different modes of the numerical test case.

We choose to display the frequency and damping error values compared to the simulation values on Figure 3a. The values are evolving with time, and here we propose to display a percentage from the true values at each time. The identification of these two parameters is better than 2%. It is interesting to underline the oscillation behavior of the different results Figures 2 and 3a. This behavior is clearly induced by the first mode and it can be observed on the other curves in smaller proportions: this is the consequence of the approximation of the Bedrosian theorem. The narrow band assumption is not completely verified.

The RMSE for this simulation is given in Figure 3b. In this numerical test case, the perfect measurement RMSE

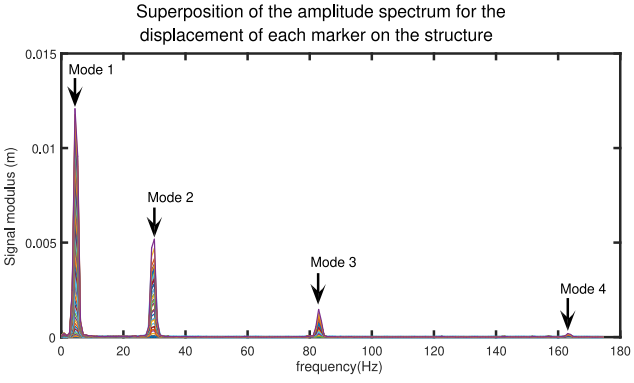

Fig. 4. Fourier Magnitude for the experimental test case data.

Table 3. Resonant modes according to Fourier analysis.

Mode number	Fourier analysis (Hz)		Our Method ending values (Hz)	
	Peak	Spectral resolution	Mean	6 × Standard deviation
1	4.408	0.87	4.720	0.06
2	29.97	0.87	29.60	0.10
3	82.87	0.87	82.92	0.18
4	163.1	0.87	163.5	0.35

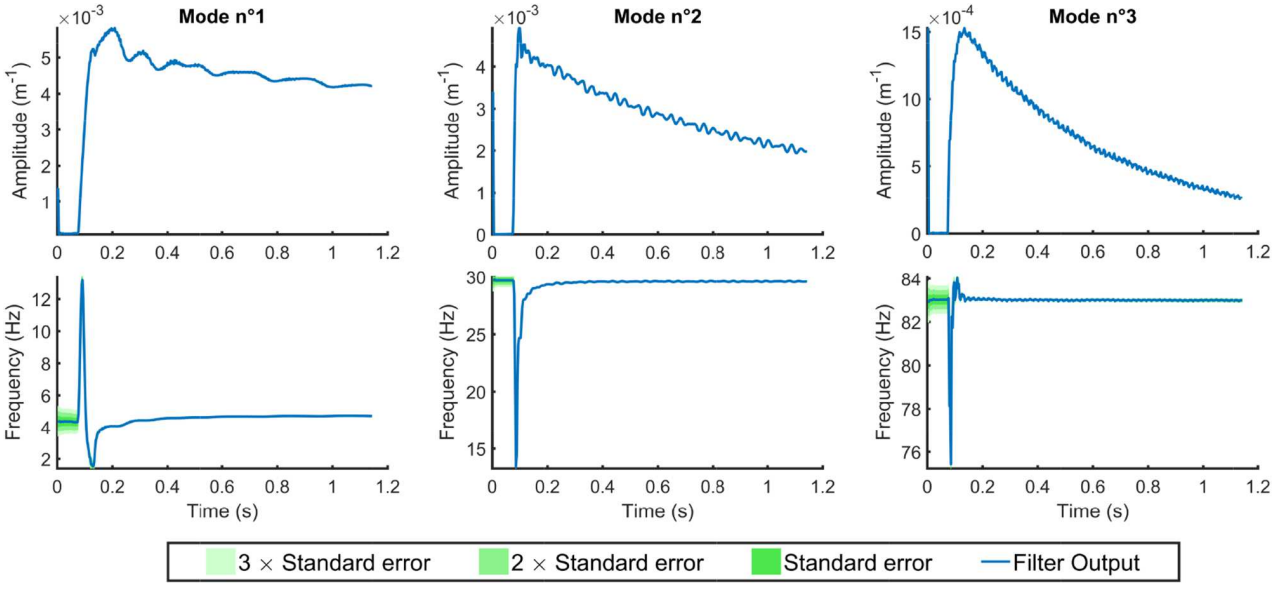

Fig. 5. Results for identification on an experimental test case.

can be displayed, this is not the case for the experimental data in Section 4.3. The RMSE converges towards the noise introduced in the numerical test case (end of the continuous line on Fig. 3b).

These results highlights the robustness of the method in the case of non stationary frequency evolution. The next part is introducing real measures acquired with a high speed camera.

4.3 Real time experimental data

4.3.1 Results on data from high speed video

The Fourier analysis (Fig. 4) show the first four natural frequencies which are compared to the identified natural frequencies Table 3. The resolution of the Fourier analysis is 0.87 Hz.

The three first modes envelop and frequency identification with the standard deviation are displayed in Figure 5.

In order to compare the results with the previous simulated ones we propose to display the RMSE but also the probability density function (PDF) of the centered errors on Figure 6. Figure 6a shows that the filter is minimizing the errors, and that the mean error level at the end of the signal is about 1×10^{-5} m is largely smaller than the GSD 1.08×10^{-4} m. Figure 6b allows to validate the Gaussian assumption used for the Kalman filter. The noise deduced from modal magnitudes is also Gaussian regardless the number of identified modes.

The results obtained are convincing in different ways. The observed parameters are invariant: the small displacements of the cantilever beam allow to keep a linear approach. Figure 6a shows that the noise chosen for the simulation is very high regarding to the real case. The identification process is performed with space resolution smaller than 1/10 of pixel resolution for vibration amplitudes. Another interesting point is that the identification process do not need to be initialized with parameters close to the good results. During the first 0.1 s the identification process is deeply disturbed before and during the shock, but converges as soon as the signals are significant regarding the noise amplitudes.

The real-time performance results are depicted in Figure 7 with the Kinematic SAMI prototyped in MatLab® language. Even if this code prototype can be improved, these results highlight the efficiency of the proposed tool for real time identification of non linear modal parameters of most of classical structures with modes in the 0 kHz–1 kHz bandwidth. The results can be seen in Figure 7.

For the sake of clarity, this article is only focusing on the signal processing part and not on the video processing part. The code is executed in a sequential way in order to simulate a real time sequential acquisition. These results

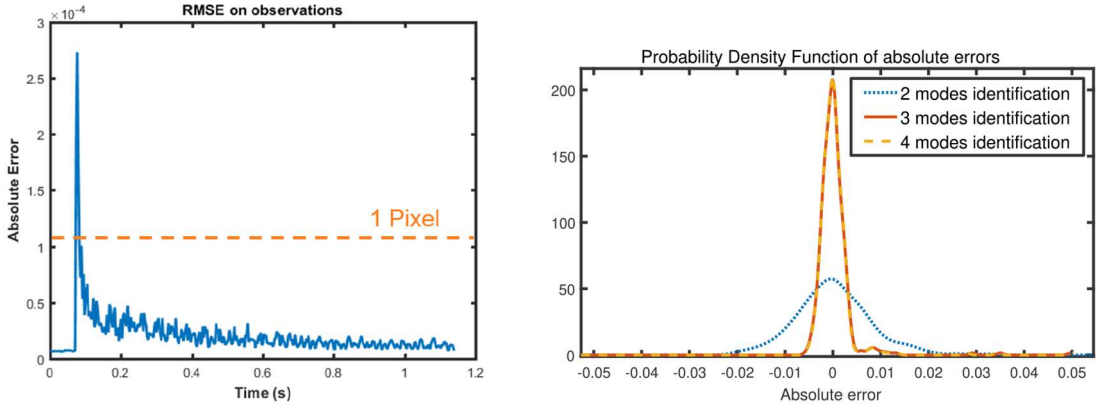

(a) RMSE ratios for identification on a nonlinear case study in case of noisy observation and perfect measurements

(b) Probability Density Function of the centered errors

Fig. 6. Two different ways to present the errors: the RMSE function of time and a centered probability density depending of the number of modes identified.

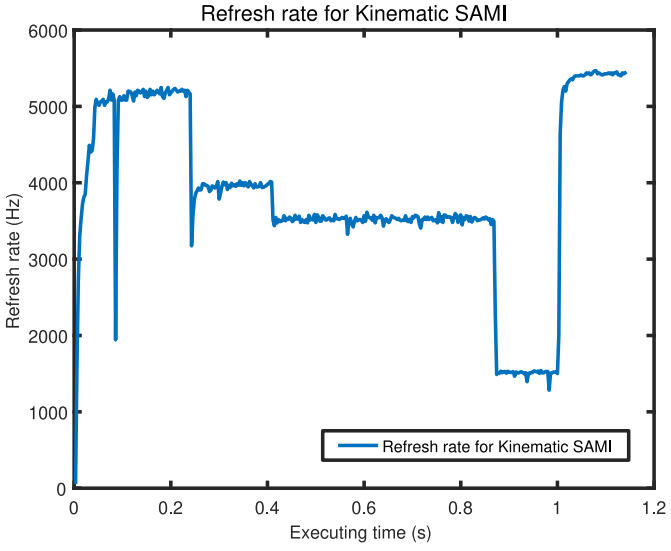

Fig. 7. Refresh frequency evolution function of time.

could be optimized later on in a real-time execution environment. The mean is varying from 1500 Hz to 5000 Hz[1]. The refresh rate depends mainly on the computing time of the innovation covariance inversion (88.6%). As the figure is not repeatable, we assume that the variation of level observed are due to the operating system activity. This frequency is high enough for MatLab® code to consider real time application applications with sample rate smaller than 1000 Hz (fps).

4.3.2 Residual analysis

The residual analysis allows to better understand the filtering process by analyzing the different contributions of the modes in the residual. Figure 8 display an absolute and normalized representation of the residual in space.

Figure 8 shows that the absolute residual has the same shape than the third mode in the case of the tracking of 2 modes. For 3 modes identification, the residual has a lower absolute error level and its space shape is not containing the third mode anymore: this experiment shows that the residual is composed of the sum of the different modes not taken into account in the reduced model. To end this residual analysis, we propose to track the fourth mode. The result is very promising because the method is able to track a very small modal amplitudes, as we can see in Figure 4. In term of residual shape, the fourth mode has a very small contribution, but can be seen with the change observed at the half of the shape residual between the 3 modes and 4 modes identifications in Figure 8. Thus, the residual shape is also an accurate tool for identifying boundary condition problems: the error is concentrated close to the clamp and highlights the difficult task to perform a perfect clamp.

5 Conclusion

In this paper, a novel method based on data assimilation has been introduced for applications on the identification of linear or nonlinear modal parameters. The method called Kinematic SAMI is designed for a real time identification of the frequencies and damping of a structure excited by shock, and is based on modal projection (time and space) of measurements performed with multi-sensors. This paper proposes specifically a real time application.

The identification method is validated first on a nonlinear system simulation and second on multiple measure points setup. This real test case is performed with high speed camera acquisition and video processing extraction on a cantilever beam. A specific residual analysis shows the efficiency of the method in the identification process for weak nonlinear modes.

[1] The processor is a Intel Core i7-412HQ @ 2.30 GHz with 16Go of RAM memory on a personal workstation.

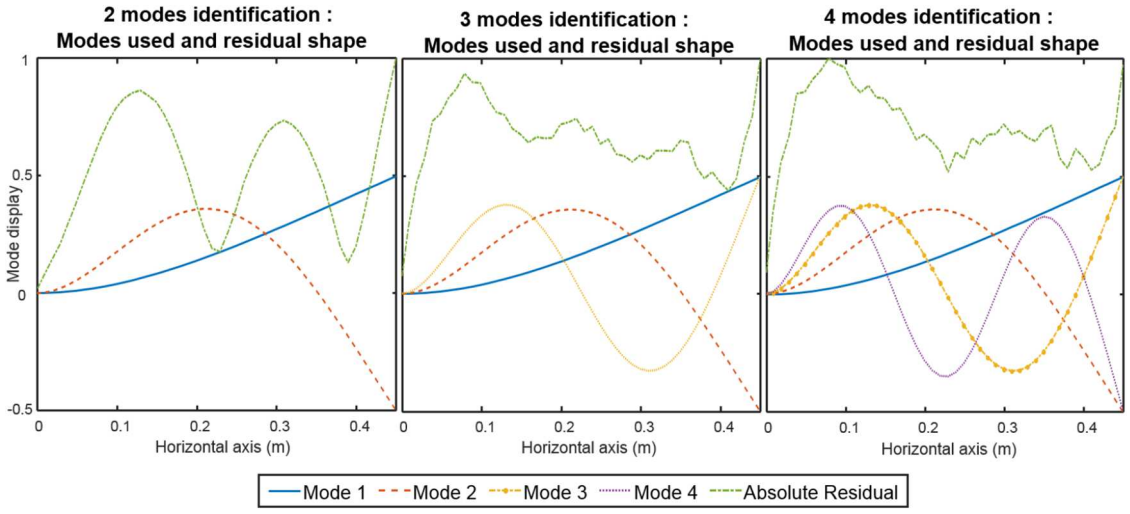

Fig. 8. Space residual display with identified mode.

Nomenclature

Symbol	Definition	Unit
a^i	Initial mode i coefficient	m
$A(t)^i$	Time depending mode i coefficient	m
C	Damping matrix	$\mathrm{kg\,s^{-1}}$
(e_x, e_y, e_z)	Space basis	
F	Evolution function	
F_{ext}	External Forces	N
F_{NL}	Nonlinear Forces	N
f^i	Frequency of the mode i	Hz
f_p	Carrier frequency	Hz
f_Δ	Phase frequency	Hz
H	Observation function	
k	Step time index	
K	Stiffness matrix	$\mathrm{kg\,s^{-2}}$
M	Mass matrix	kg
$m(t)$	Bandwidth modulation of the signal	
$P_{k\|k-1}$	Covariance of state vector at step k knowing step $k-1$	
Q_k	Process noise covariance	
R_ν	Covariance matrix of ν	N
S	Shape function depending of the 3 axis position variables	m
t	Time	s
$\hat{q}$	Generalized coordinate vector	m
V^i	Temporal modal contribution of mode i	m
$\mathcal{V}^i$	Hilbert transform of V^i	
v_k	Observation noise (vector)	m
w_k	Process noise (vector)	
X_k	State vector at step k	
x	x position	m
$\dot{x}$	Speed on x axis	$\mathrm{m\,s^{-1}}$
y	y position	m
z	z position	m
Z_k	Observation vector	
Δt	Step time $t = k \cdot \Delta t$	s
ν	Uncertainty of the model	N
μ	Uncertainty of the model	N
Φ	Modal basis	
ϕ^i	Phase of the mode i	m
ω	System Pulsation	$\mathrm{rad\,s^{-1}}$
σ_{sim}	Standard deviation	m
ξ^i	Damping of the mode i	

This research is funded by a Ph.D. grant of the French National Technological Research Agency (ANRT) and Vannier-Kinoptik, a french company specialized in high speed cameras through the FAst MOving SYStem (FAMOSYS) project.

References

[1] N.M.M. Maia, J.M.M. Silva, Theoretical and Experimental Modal Analysis, Engineering Dynamics Series, Research Studies Press, Boston, 1997
[2] D.J. Ewins, Modal Testing: Theory, Practice, and Application, Mechanical Engineering Research Studies: Engineering Dynamics Series, Research Studies Press, Boston, 2000
[3] G. Bissinger, D. Oliver, 3-D laser vibrometry on legendary old Italian violins, Sound Vib. **41**, 10–15 (2007)
[4] H. Marschner, Fritz Rischbieter, Three-Dimensional Operational Deflection Shape Analysis of Squealing Disc Brakes, in SAE Technical Paper, SAE International, October 2004.
[5] G. Kerschen, M. Peeters, J.C. Golinval, C. Stéphan, Nonlinear modal analysis of a full-scale aircraft, J. Aircraft **50**, 1409–1419 (2013)
[6] E. Blayo, M. Bocquet, J. Vernon, L'assimilation de données, un outil de synthèse de l'information, June 9
[7] R.E. Kalman, A new approach to linear filtering and prediction problems, J. Basic Eng. **82**, 35–45 (1960)
[8] R.E. Kalman, Contributions to the theory of optimal control, Bol. Soc. Mat. Mex. **5**, 102–119 (1960)
[9] G.L. Smith, S.F. Schmidt, L.A. McGee, Application of statistical filter theory to the optimal estimation of position and velocity on board a circumlunar vehicle. Technical Report R-135, National Aeronautics and Space Administration, 1962
[10] Analytic Sciences Corporation and A. Gelb, Applied Optimal Estimation, M.I.T. Press, Cambridge, MA, 1974

[11] G.M. Siouris, G. Chen, J. Wang, Tracking an incoming ballistic missile using an extended interval Kalman filter, IEEE Trans. Aerosp. Electron. Syst. **33**, 232–240 (1997)
[12] G.P. Huang, A.I. Mourikis, S.I. Roumeliotis, Analysis and improvement of the consistency of extended Kalman filter based SLAM, in IEEE International Conferenc on Robotics and Automation, 2008, pp. 473–479
[13] S.E. Azam, E. Chatzi, C. Papadimitriou, A. Smyth, Experimental validation of the Kalman-type filters for online and real-time state and input estimation. J. Vib. Control **23**, 2494–2519 (2015)
[14] C.-K. Ma, D.-C. Lin, J.-M. Chang, Estimation of forces generated by a machine mounted upon isolators under operating conditions. J. Franklin Inst. **336**, 875–892 (1999)
[15] C.-K. Ma, C.-C. Ho, An inverse method for the estimation of input forces acting on non-linear structural systems. J. Sound Vib. **275**, 953–971 (2004)
[16] P.J. Kootsookos, A review of the frequency estimation and tracking problems, 1993
[17] J. Antoni, L. Garibaldi, S. Marchesiello, M. Sidhamed, New separation techniques for output-only modal analysis. Shock Vib. **11**, 227–242 (2004)
[18] D. Simon, Optimal State Estimation: Kalman, H Infinity, and Nonlinear Approaches, Wiley-Interscience, New York, 2006
[19] Y. Shao, C.K. Mechefske, Gearbox vibration monitoring using extended Kalman filters and hypothesis tests, J. Sound Vib. **325**, 629–648 (2009)
[20] D.A. Ehrhardt, M.S. Allen, Measurement of nonlinear normal modes using multi-harmonic stepped force appropriation and free decay. Mech. Syst. Signal Process. **76-77**, 612–633 (2016)
[21] Y. Yang, C. Dorn, T. Mancini, Z. Talken, G. Kenyon, C. Farrar, D. Mascareñas, Blind identification of full-field vibration modes from video measurements with phase-based video motion magnification, Mech. Syst. Signal Process. **85**, 567–590 (2017)
[22] M. Abdollahpouri, G. Takács, B. Rohaľ-Ilkiv, Real-time moving horizon estimation for a vibrating active cantilever, Mech. Syst. Signal Process. **86**, 1–15 (2017)
[23] Z. Dzunic, J.G. Chen, H. Mobahi, O. Büyüköztürk, J.W. Fisher, A Bayesian state-space approach for damage detection and classification. Mech. Syst. Signal Process. **96**, 239–259 (2017)
[24] F. Naets, F. Cosco, W. Desmet, An extended Kalman filter approach for augmented strain/stress visualization in mechanical systems, in 2014 IEEE/ASME 10th International Conference on Mechatronic and Embedded Systems and Applications (MESA), September 2014 pp. 1–6
[25] J.-L. Dion, C. Stephan, G. Chevallier, H. Festjens, Tracking and removing modulated sinusoidal components: A solution based on the kurtosis and the Extended Kalman Filter, Mech. Syst. Signal Process. **38**, 428–439 (2013)
[26] Y.-J. Cha, J.G. Chen, O. Büyüköztürk, Output-only computer vision based damage detection using phase-based optical flow and unscented Kalman filters. Eng. Struct. **132**, 300–313 (2017)
[27] V. Ondra, I.A. Sever, C.W. Schwingshackl, A method for detection and characterisation of structural non-linearities using the Hilbert transform and neural networks, Mech. Syst. Signal Process. **83**, 210–227 (2017)
[28] A. Goeller, J.L. Dion, R.L. Breton, T. Soriano, B. Roux, Dynamic system stochastic identification mixed with video processing: Validation on a real case, in Mechatronics (MECATRONICS)/11th France-Japan & 9th Europe-Asia Congress & 17th International Conference on Research and Education in Mechatronics (REM), 2016, pp. 146–151
[29] M. Bocquet, Introduction to the principles and methods of data assimilation in geosciences, Technical report, École des Ponts ParisTech, February 2014
[30] N. Peyret, J.-L. Dion, G. Chevallier, A framework for backbone experimental tracking: Piezoelectric actuators, stop-sine signal and Kalman filtering. Mech. Syst. Signal Process. **78**, 28–42 (2016)
[31] E. Bedrosian, A product theorem for Hilbert transforms, Proc. IEEE **51**, 868–869 (1963)
[32] C. Pachaud, T. Gerber, M. Firla, N. Martin, C. Mailhes, Consequences of non-respect of the Bedrosian theorem when demodulating, in The Tenth International Conference on Condition Monitoring and Machinery Failure Prevention Technologies (CM2013), 2013
[33] M.R. Shahriar, P. Borghesani, R.B. Randall, A.C.C. Tan, An assessment of envelope-based demodulation in case of proximity of carrier and modulation frequencies, Mech. Syst. Signal Process. **96**, 176–200 (2017)
[34] A. Goeller, Contribution à La Perception Augmentée de Scènes Dynamiques : Schémas Temps Réels d'assimilation de Données Pour La Mécanique Du Solide et Des Structures. PhD thesis, 2018
[35] Z. Zhang, A flexible new technique for camera calibration. IEEE Trans. Pattern Anal. Mach. Intell. **22**, 1330–1334 (2000)

Cite this article as: A. Goeller, J.-L. Dion, R.L. Breton, T. Soriano, Kinematic SAMI : a new real-time multi-sensor data assimilation strategy for nonlinear modal identification, Mechanics & Industry **21**, 413 (2020)